Carbohydrate Polymers **22** (1993) 175–186

Thermogelation of methylcellulose. Part II: effect of hydroxypropyl substituents

Anwarul Haque, Robert K. Richardson, Edwin R. Morris*

Department of Food Research & Technology, Cranfield University, Silsoe College, Silsoe, Bedford, UK, MK45 4DT

Michael J. Gidley & David C. Caswell

Unilever Research, Colworth Laboratory, Sharnbrook, Bedford, UK, MK44 1LQ

(Received 26 June 1993; accepted 12 July 1993)

Thermogelation of hydroxypropylmethylcellulose (HPMC) samples (E4M, F4M and K4M from Dow) follows the two-stage mechanism observed previously for methylcellulose (A4M) and attributed to dissociation of cellulosic 'bundles' as a necessary precursor to hydrophobic association. All four samples show the same unusual form of shear thinning, indicating similar macromolecular organisation in solution. The hydroxypropyl substituents in HPMC, however, appear to inhibit intermolecular association since, in comparison with A4M, the proportion of visible high-resolution ^{1}H-NMR signal in the solution state is higher, thermogelation does not occur until higher temperature, and the resulting gels are substantially weaker. Thermal 'demixing' of Klucel, a highly substituted hydroxypropylcellulose from Hercules, occurs at essentially the same temperature as resolubilisation on cooling, supporting the conclusion that the thermal hysteresis observed between formation and dissociation of methylcellulose and HPMC gels arises from melting and re-formation of the postulated 'bundle' structure, and not from hydrophobic interactions.

INTRODUCTION

The present investigation arose from work on production of gluten-free bread from rice flour, using hydroxypropylmethylcellulose (HPMC) (K4M from Dow) as one of the structuring agents (Haque *et al.*, 1993). The temperature course of thermogelation was found to be unexpectedly complex, prompting a detailed study of a simpler Dow product (A4M), in which substitution is confined to methyl groups. The results are reported in the preceding paper (Haque & Morris, 1993).

The main conclusion was that methylcellulose (A4M) exists in solution as aggregated 'bundles', held together by packing of unsubstituted or sparingly substituted regions of cellulosic structure, and by hydrophobic clustering of methyl groups in regions of denser substitution. As the temperature is raised, the ends of the bundles come apart, exposing methyl groups to the aqueous environment and causing a large increase in volume (with consequent increase in elastic modulus, G'). At higher temperature the methyl substituents shed structured water, and form a hydrophobically cross-linked network (leading to a second 'wave' of increase in G'). We now report the behaviour observed for HPMC samples, in which the methyl group remains the dominant substituent, but is augmented by smaller amounts of the larger and more polar hydroxypropyl group, with substantial modification of functional properties in practical applications (Greminger & Savage, 1973; Sarkar, 1979; Grover, 1986).

MATERIALS AND METHODS

The samples studied were A4M, E4M, F4M and K4M from the Methocel range of cellulose derivatives produced by the Dow Chemical Company. In each case, '4M' denotes a solution viscosity of 4 Pa s measured under standard conditions in a capillary viscometer. The initial letter 'A' denotes methylcellulose; 'E', 'F' and 'K' correspond to hydroxypropylmethyl derivatives with different levels of incorporation of the two substituents within the ranges shown in Table 1. Precise analytical

*To whom correspondence should be addressed.

Carbohydrate Polymers 0144-8617/93/$06.00

Table 1. Composition[a] and enthalpy values for Methocel cellulose derivatives

Material	ΔH (J/g)	Average number of substituents per residue	
		Methoxyl	Hydroxypropyl
A4M	16	1·6–1·9	0
E4M	15	1·8–2·0	0·20–0·31
F4M	15	1·7–1·9	0·10–0·20
K4M	4	1·1–1·6	0·10–0·30

[a]Composition ranges from Dow technical literature.

Table 2. Composition of Methocel samples used in the present work[a]

Sample	Batch no.	Methoxyl DS	Hydroxypropyl MS
A4M	MM88051912A	1·81	0·00
E4M	MM8908603E	1·88	0·21
K4M	MM90092303K	1·40	0·22

[a]Dr N. Sarkar, pers. comm., 1992.

values for the production batches of A4M, E4M and K4M used in the present work were kindly supplied by Dr N. Sarkar of Dow, and are listed in Table 2. The same information was not, unfortunately, available for F4M, but, as detailed below, its behaviour was found to be virtually identical to that of the well characterised E4M sample. Some comparative studies were also made using hydroxypropylcellulose (Klucel) from Hercules. The experimental procedures used were identical to those described in the preceding paper (Haque & Morris, 1993).

THERMAL DEMIXING OF HYDROXYPROPYLCELLULOSE

As a prelude to investigation of the effect of low levels of hydroxypropyl substitution in methylcelluloses, a brief study was first made of a commercial cellulose derivative (Klucel) in which the hydroxypropyl group is the sole substituent and is present as a major component of the polymer. Klucel has a molar substitution of 4·0, with DS ≈ 2·6 (pers. comm., 1992, Dr E. Just, Worldwide Director of R & D, Hercules Inc.), so that, on average, only 0·4 of the three available hydroxyl groups per sugar ring (i.e. ~13%) remain unsubstituted. Unlike Methocels, solutions of Klucel do not gel on heating; instead, the polymer 'demixes' into a flocculated dispersion, which re-dissolves on cooling (Klug, 1971).

Figure 1 shows the temperature dependent changes in rheology observed on heating and cooling a solution of Klucel (2% (w/v)). Thermal demixing is marked by a sharp decrease in both G' and G'' at ~45°C. At higher temperatures the moduli rise again and then level out, with the initial increase being particularly evident in G'. However, since the system is then a heterogeneous dispersion, the detail of these changes is unlikely to be

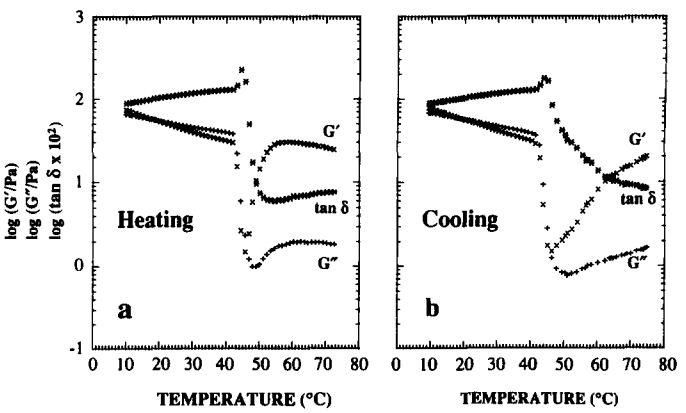

Fig. 1. Temperature dependent changes in G' (×), G'' (+) and tan δ (*) for Klucel (2% (w/v)) on (a) heating and (b) cooling at 1 deg min^{-1}. Measurements were made at 10 rad s^{-1} and 0·5% strain.

of any fundamental significance. Quantitative recovery of the initial solution rheology is observed on cooling (Fig. 1(b)), with the midpoint temperatures of the mixing and demixing processes showing only very slight hysteresis (~1°C, which may be due, at least in part, to thermal lag).

Both processes are accompanied (Fig. 2) by sharp thermal transitions in DSC (exothermic mixing on cooling; endothermic demixing on heating). As shown in Fig. 3, the transition-midpoint temperatures are independent of concentration (for 0·5% and 2% (w/v)) and extrapolate to virtually the same value at zero scan rate ($T_m \approx 46{\cdot}5$°C on heating and ≈45·5°C on cooling), in good agreement with the rheological changes shown in Fig. 1.

The values of ΔH for the heating and cooling processes agree closely and, as would be expected, are independent of scan rate (Fig. 3). A recent detailed study of hydroxypropylcellulose fractionated to a narrow distribution of molecular weight (Robitaille *et al.*, 1991) showed a linear reduction in ΔH with increasing concentration, due to formation of a cholesteric mesophase in concentrated solution. The experimental values extrapolated to zero at ~67% (w/w), and

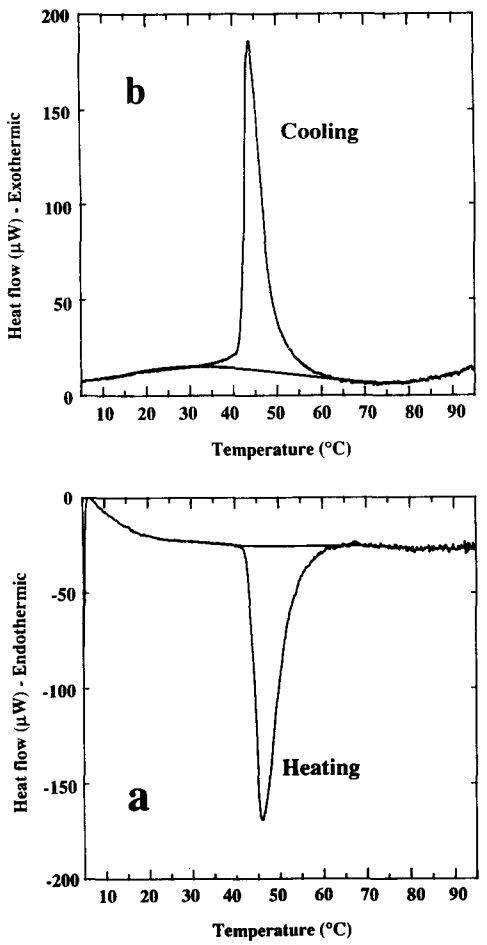

Fig. 2. Illustrative DSC traces for Klucel (2% (w/v)) on (a) heating and (b) cooling at 0·1 deg min^{-1}.

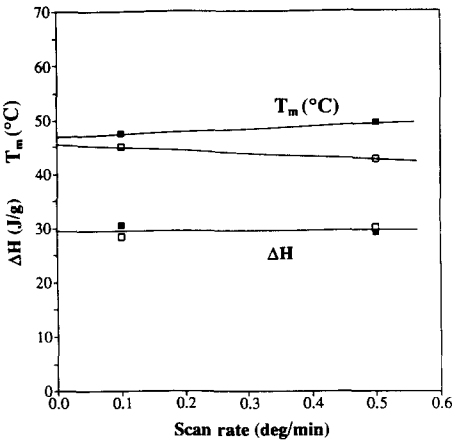

Fig. 3. Enthalpy changes (ΔH) and transition-midpoint temperatures (T_m) from DSC for 2% (w/v) Klucel on heating (■) and cooling (□) at 0·1 and 0·5 deg min^{-1}.

the maximum limiting value of ΔH obtained by extrapolation to zero concentration was ~27·4 J g^{-1}, in good agreement with the value observed (Fig. 3) for the more dilute solutions studied in the present work (ΔH = 29·5 ± 1 J g^{-1} at 2% (w/v)).

Figure 4 shows the mechanical spectrum obtained for 2% (w/v) Klucel in the solution state at 25°C. The behaviour is closely similar to that observed for underivitised polysaccharide coils at concentrations above the onset of coil overlap and entanglement (see for example Morris, 1984). Liquid-like response dominates at low frequency, with $G'' \gg G'$ and a Newtonian plateau in η^*, but at higher frequency G' exceeds G'' and η^* falls.

Shear-thinning is also evident in rotational measurements of steady-shear viscosity (Fig. 5(a)). The shear-rate ($\dot{\gamma}$) dependence of viscosity (η) for underivitised

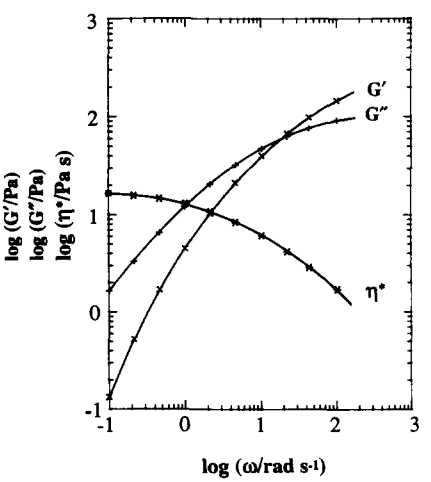

Fig. 4. Mechanical spectrum (0·5% strain) for 2% (w/v) Klucel at 25°C, showing the frequency (ω) dependence of G' (×), G'' (+) and η^* (*).

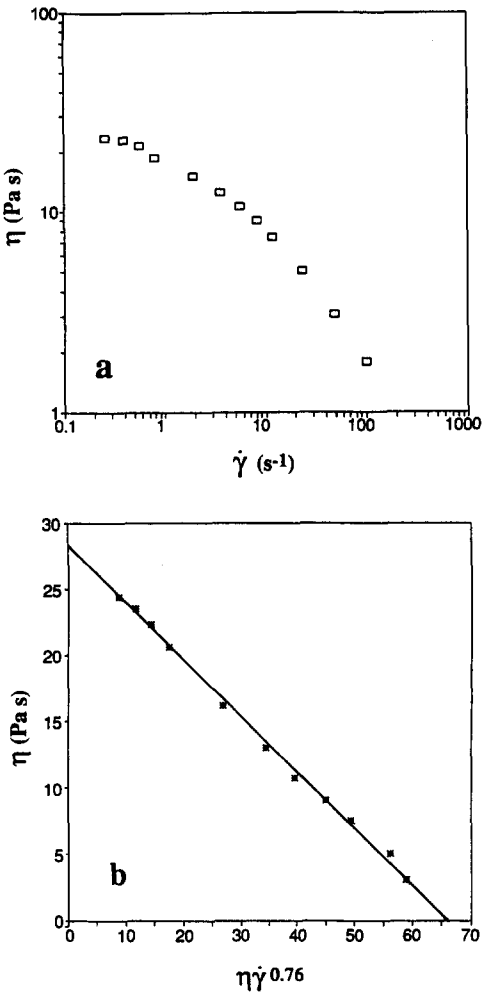

Fig. 5. Variation of viscosity (η) with shear rate ($\dot{\gamma}$) for 2% (w/v) Klucel at 25°C plotted (a) in conventional double-logarithmic form, and (b) in a form that gives linearity for disordered polysaccharides interacting only by physical entanglement (Morris, 1990).

polysaccharide coils can be fitted, with good precision (Morris, 1990), to the relationship:

$$\eta = \eta_0/[1 + (\dot{\gamma}/\dot{\gamma}_{1/2})^p] \quad (1)$$

where η_0 is the maximum 'Newtonian' viscosity at low shear rate; $\dot{\gamma}_{1/2}$ is the shear rate at which $\eta = \eta_0/2$; and p has a constant (empirical) value of 0·76. Equation (1) can be rearranged as a linear relationship between η and $\eta\dot{\gamma}^p$:

$$\eta = \eta_0 - [(1/\dot{\gamma}_{1/2})^p]\eta\dot{\gamma}^p \quad (2)$$

giving straight-line graphs of η versus $\eta\dot{\gamma}^{0.76}$. The results obtained for Klucel (Fig. 5(a)) show good linearity when plotted in the same way (Fig. 5(b)).

In summary, therefore, the main conclusions from this brief investigation of Klucel are that it shows normal 'random coil' behaviour in solution and that formation and dissociation of hydrophobic clusters occur at essentially the same temperature. In both these respects it differs from methylcellulose (A4M), consistent with the proposal (Haque & Morris, 1993) that the thermal hysteresis and unusual shear thinning of A4M arise from unsubstituted or sparingly substituted chain sequences, which would, of course, be essentially abolished at the much higher degree of substitution in Klucel.

THERMOGELATION OF HPMC

Preliminary comparison with methylcellulose (A4M)

Figure 6 shows the temperature dependence of tan δ (the ratio of liquid-like to solid-like response) for solutions of A4M, E4M and K4M (2% (w/v)) heated at constant rate (1 deg min^{-1}). All three plots have the same general form, with two distinct 'waves' of structure-formation (i.e. regions of reduction in tan δ) after the initial shallow increase, but they are offset to different ranges of temperature. Thermogelation of K4M occurs about 20 degrees higher than for A4M, as might be anticipated from its lower content of hydrophobic substituents (Table 2). The gelation temperature of E4M, although lower than that of K4M, is, however, also higher than for A4M, despite having a higher methoxyl DS (1·88, in comparison with 1·81 for A4M), indicating that incorporation of small amounts of hydroxypropyl substituents inhibits hydrophobic gelation.

Methocel K4M

Since K4M was the material used in the baking trials that prompted this work (Haque *et al.*, 1993), it was studied in somewhat greater detail than the other HPMC samples. Figure 7 shows mechanical spectra for 3% (w/v) K4M in the solution state (at 25°C), in the gel

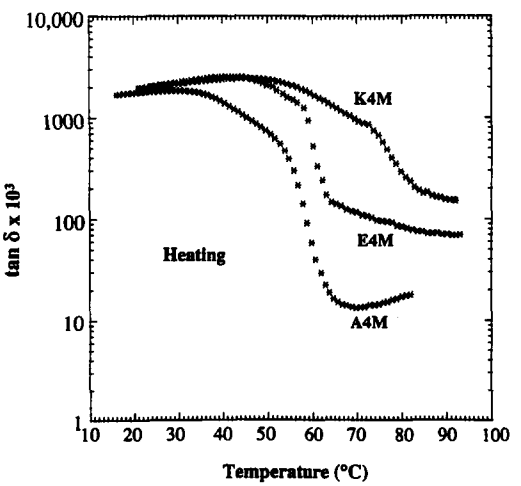

Fig. 6. Temperature course of thermogelation for Methocel samples A4M, E4M and K4M (2% (w/v)), monitored by changes in tan δ (10 rad s^{-1}; 1% strain).

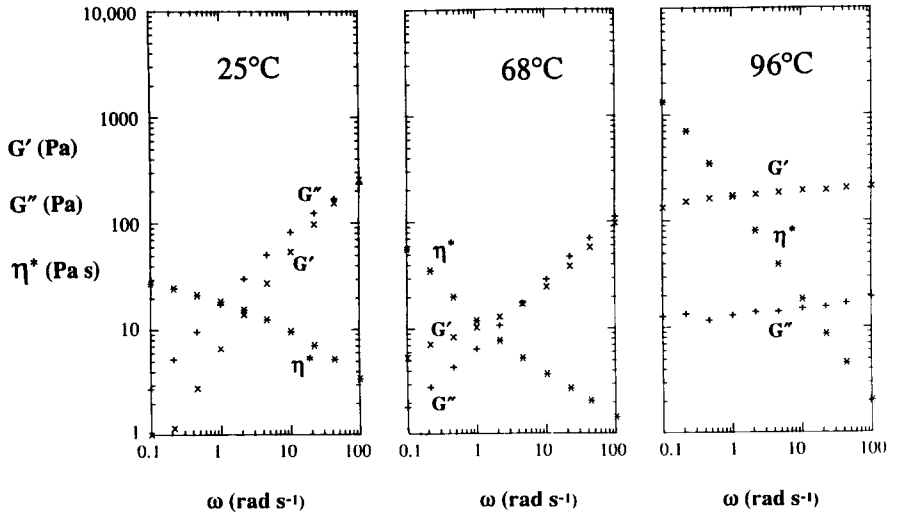

Fig. 7. Mechanical spectra (1% strain) for 3% (w/v) K4M at 25, 68 and 96°C, showing the progressive change in the frequency (ω) dependence of G' (×), G'' (+) and η^* (*).

state (at 96°C), and at an intermediate temperature (68°C) close to completion of the first 'wave' of structure-formation in Fig. 6. The spectra are closely similar in form to corresponding plots for A4M (Haque & Morris, 1993). As shown in Fig. 8, however, the gel strength (G') for K4M is substantially lower than for corresponding concentrations of A4M (by about a factor of 30), again indicating the antagonistic effect of hydroxypropyl groups.

The temperature-course of rheological change on heating and cooling is illustrated in Fig. 9. As in the case of A4M, there is substantial thermal hysteresis between formation and dissociation of the hydrophobic gel. The variation in G' and G'' (at 10 rad s^{-1}) throughout the thermogelation process is shown in Fig. 10 for K4M concentrations of 1, 2, 3 and 6% (w/v). The curves are broadly similar to those obtained for A4M (Haque & Morris, 1993), but the characteristic dip in G'', marking the onset of the second (major) 'wave' of structure-formation, is more pronounced, displaced to higher temperature, and accompanied, at the higher concentrations, by a smaller dip in G'. Although the relative magnitude of the various temperature dependent changes varies considerably with concentration, they show no significant changes in position, indicating that, as for A4M, the temperature-course of thermogelation is essentially independent of polymer concentration.

The first increase in G', which is very evident at 1% (w/v) (Fig. 10(a)), becomes progressively obscured at higher concentrations by the contribution from entanglement-coupling in solution. When measurements are made at lower frequency (0·1 rad s^{-1}), however, the two separate 'waves' of increase in G' are again clearly

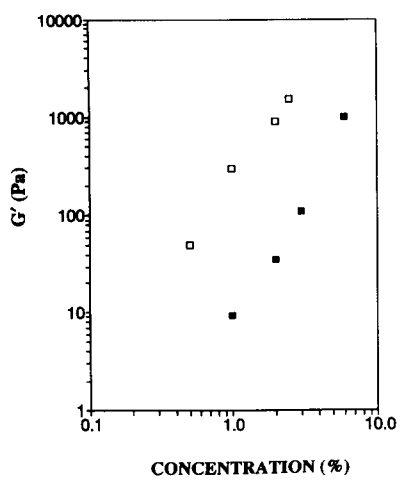

Fig. 8. Comparison of the concentration dependence of G' (10 rad s^{-1}; 1% strain) for methylcellulose (□) and HPMC (■), illustrated for A4M (72°C) and K4M (92°C).

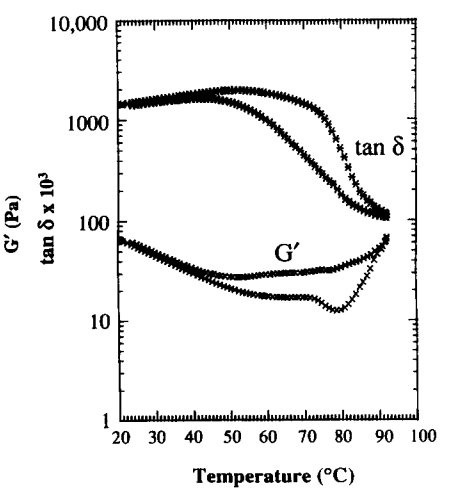

Fig. 9. Thermal hysteresis in formation and dissociation of HPMC gels, illustrated for 3% (w/v) K4M. G' (×) and tan δ (*) were measured at 10 rad s^{-1} and 1% strain.

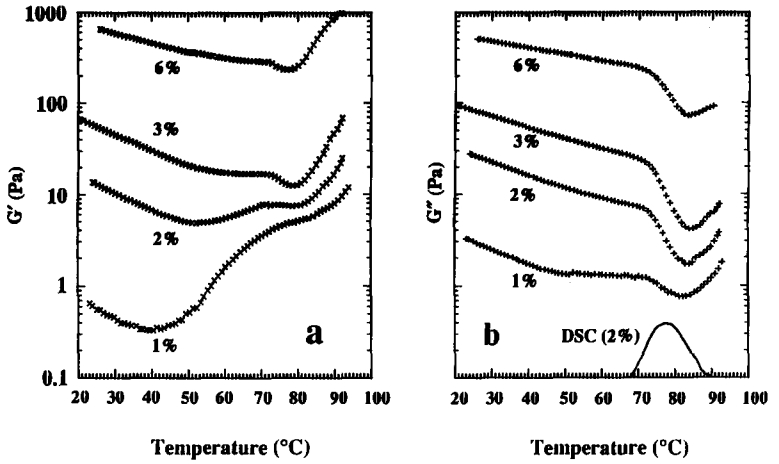

Fig. 10. Temperature course of thermogelation for 1, 2, 3 and 6% (w/v) K4M, monitored by changes in (a) G' and (b) G'' at 10 rad s^{-1} and 1% strain. The temperature course of thermal change in DSC (Fig. 14) is included for direct comparison.

visible, as illustrated in Fig. 11 for 3% (w/v) K4M. The sharp decrease in G'' at high frequency (10 rad s^{-1}; Fig. 10) is replaced at lower frequency by an increase in modulus (Fig. 11(b)), indicating that it comes from formation of stable crosslinks at the expense of topological interactions. Figure 1(1a) indicates that the slight dip in the temperature-course of G' at higher frequency (Fig. 10(a)) arises in a similar way.

E4M and F4M

Figure 12 shows mechanical spectra for 2% (w/v) E4M and F4M at 25°C (in the solution state), 58°C (towards completion of the first wave of structure-formation in Fig. 6), and 82°C (after thermogelation). The spectra are closely similar to those shown in Fig. 7 for K4M. The temperature course of rheological change during thermogelation on heating and reversion to the solution state on cooling is shown in Fig. 13. The behaviour of E4M and F4M is virtually identical in all cases.

The sharp decrease in G'' and accompanying slight dip in G' observed for K4M (Fig. 10) are again evident

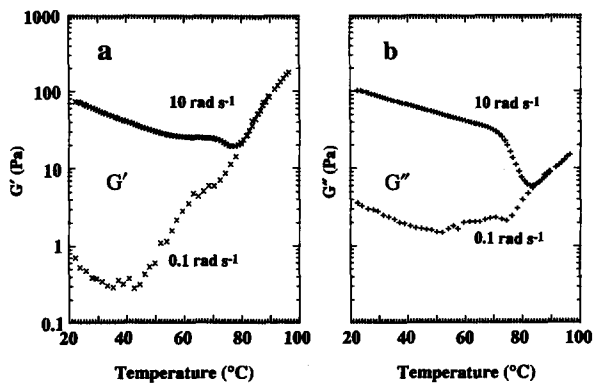

Fig. 11. Temperature course of thermogelation for 3% (w/v) K4M, monitored by changes in (a) G' and (b) G'' (0·5% strain) at 10 and 0·1 rad s^{-1}.

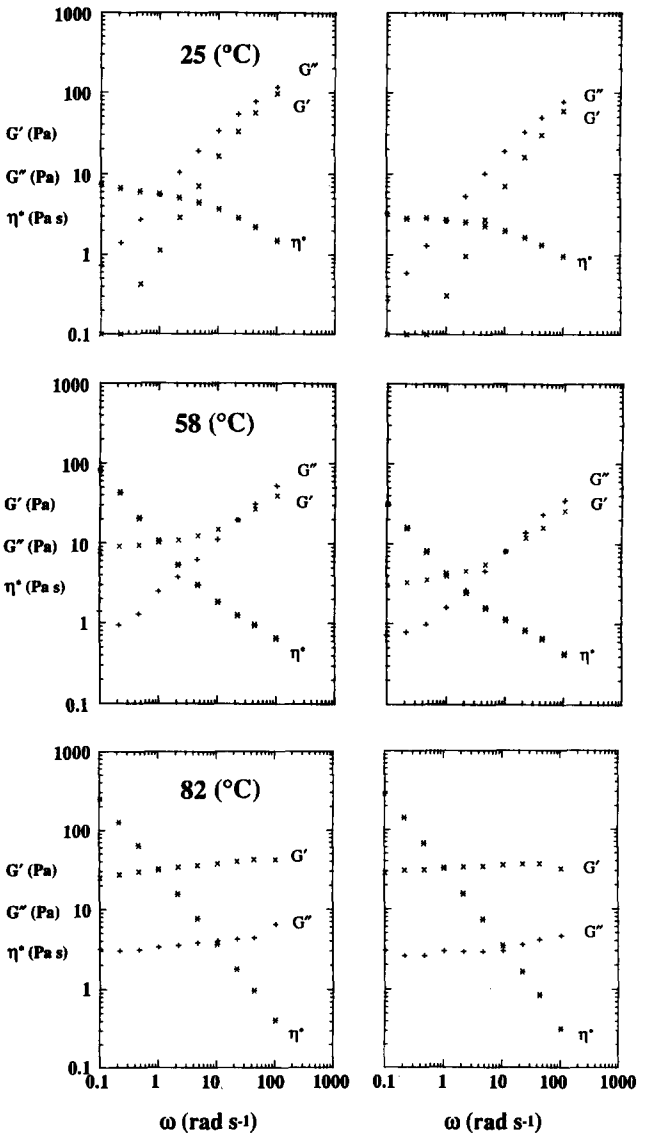

Fig. 12. Mechanical spectra (2% (w/v); 10 rad s^{-1}; 1% strain) for E4M (left) and F4M (right), at 25°C (top), 58°C (middle) and 82°C (bottom), showing the variation of G' (×), G'' (+) and η^* (*) with frequency (ω).

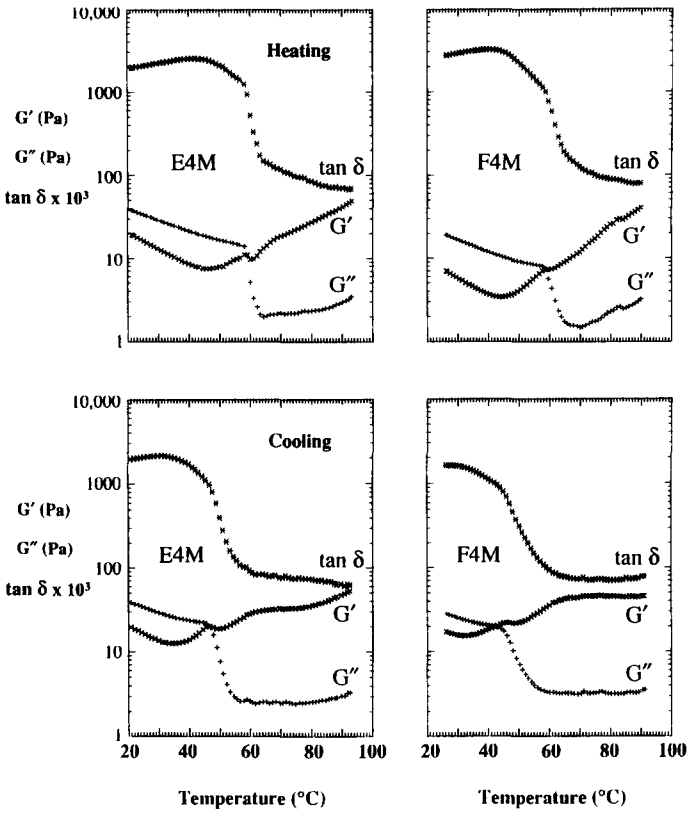

Fig. 13. Temperature course of thermogelation (top) and network dissociation (bottom) for E4M (left) and F4M (right). Symbols and conditions as in Fig. 12.

in the heating scans shown in Fig. 13 (upper traces). The involvement of two separate mechanisms of structuring is shown particularly clearly by the variation in G' on cooling (Fig. 13; lower traces).

DIFFERENTIAL SCANNING CALORIMETRY

Figure 14 shows illustrative DSC plots for E4M, F4M and K4M on heating and cooling at very slow scan rate (0·1 deg min^{-1}) where thermal lag is negligible. All three materials give a single endotherm on heating and a single exotherm on cooling, with substantial thermal hysteresis. As illustrated in Fig. 10, the thermal changes are confined to the temperature range of the second major 'wave' of structure-formation.

The heating scans for E4M and F4M are virtually identical, consistent with the close similarity in rheological properties shown in Figs 12 and 13. The relative positions (Fig. 14) of the endotherms for A4M (Haque & Morris, 1993), E4M and K4M agree well with the temperature dependence of thermogelation (Fig. 6). In each case, absorption of heat begins at the same temperature as the sharp (second) decrease in tan δ; this is also the temperature at which the samples becomes visually opaque.

The cooling exotherms for E4M, F4M and K4M, although showing appreciable differences in shape, all span approximately the same range of temperature (from ~70 to ~45°C) and are comparable in width to the first exothermic process observed for A4M, but displaced to higher temperature by about 20°C. In terms of the argument developed in the preceding paper (Haque & Morris, 1993), these peaks would be attributed to the heat released by formation of water 'cages' around hydrophobic substituents exposed to the aqueous environment on dissociation of the gel network.

The second exotherm observed for A4M, and attributed to enthalpic interactions within cellulosic 'bundles', is undetectable for the other samples, implying that hydroxypropyl substituents cause a major reduction in the enthalpic stability of the bundles. This conclusion is supported by recent studies using ethylene glycol to provide a more compatible solvent-environment for hydrophobic substituents. Addition of ethylene glycol to solutions of A4M caused a progressive increase in G' (Haque *et al.*, 1994), indicating partial dissociation of the bundles towards the 'swollen' state attained in water only after heating to ~55°C (i.e. at the end of the first 'wave' of increase in G'). The concentration of ethylene glycol required to completely eliminate the first 'wave' for A4M was ~40% (v/v). The corresponding value for K4M (Jones, 1992) is much lower (~10% (v/v)), again suggesting a less stable 'bundle' structure.

Transition-midpoint temperatures and ΔH values for DSC heating and cooling scans at different scan-rates and different concentrations of polymer are listed in

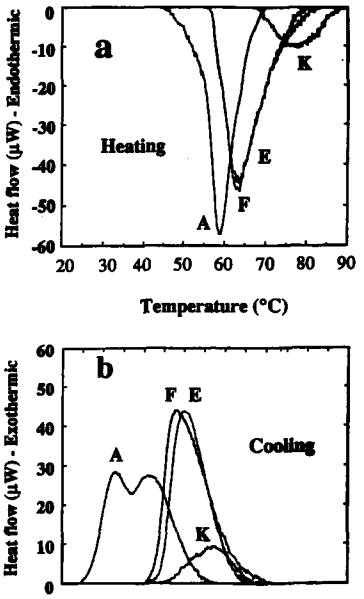

Fig. 14. DSC traces, after baseline subtraction, for 2% (w/v) A4M, E4M, F4M and K4M on (a) heating and (b) cooling at 0·1 deg min^{-1}.

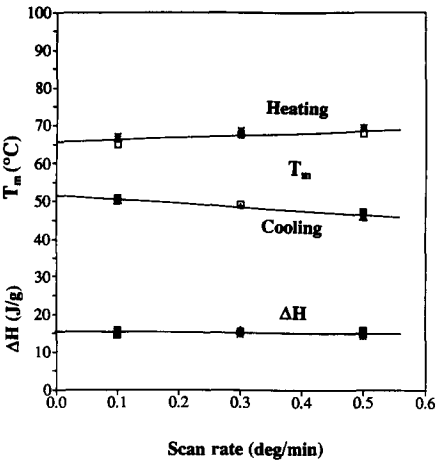

Fig. 15. Scan-rate dependence of transition-midpoint temperatures (T_m) and enthalpy changes (ΔH) from DSC, illustrated for F4M at concentrations (% (w/v)) of 0·5 (*), 1 (▲), and 2·0 (□).

Table 3, and extrapolation to zero scan rate is illustrated in Fig. 15. The extrapolated values are given in Table 4. As in the rheological studies reported above, results for E4M and F4M are closely similar. The T_m values for K4M are appreciably higher and show greater thermal hysteresis. The most striking difference, however, is that K4M has a much smaller ΔH value than the other three samples, presumably due to its lower degree of substitution (Table 1), with a consequent reduction in the structuring of water around the polymer chains (Tanford, 1980; Franks, 1983).

Table 3. Enthalpy changes (ΔH) and transition-midpoint temperatures (T_m) from DSC for Methocel HPMC samples E4M, F4M and K4M. Corresponding values for methylcellulose (Methocel A4M; Haque & Morris, 1993) are included for direct comparison

Methocel sample	Concentration (% (w/v))	Scan-rate (deg min^{-1})	T_m (°C)		ΔH	
			Heating	Cooling	Heating	Cooling
A4M	0·5	0·1	60·9	36·6	−15·0	16·7
		0·5	65·1	34·6	−15·7	15·9
	2·0	0·1	59·2	38·8	−15·5	16·3
		0·5	62·3	35·1	−15·6	16·3
E4M	0·5	0·1	65·1	50·5	−15·0	16·7
		0·5	67·7	48·5	−15·7	15·9
	2·0	0·1	64·8	51·5	−15·5	16·3
		0·5	67·3	48·5	−15·6	16·3
F4M	0·5	0·1	66·9	50·8	−14·5	15·4
		0·3	68·6	48·0	−14·9	15·3
		0·5	69·5	47·3	−14·3	15·5
	1·0	0·1	66·7	50·4	−14·8	15·4
		0·3	68·4	48·4	−15·9	15·9
		0·5	69·4	45·9	−15·0	15·7
	2·0	0·1	64·9	50·9	−15·9	15·3
		0·3	67·6	49·4	−15·6	15·3
		0·5	67·7	47·0	−15·9	15·2
K4M	0·5	0·1	78·5	56·3	−4·0	4·3
		0·3	81·1	54·9	−4·2	4·1
		0·5	82·0	51·7	−4·2	4·3
	1·0	0·1	75·5	56·5	−4·1	4·3
		0·3	78·1	54·9	−4·1	4·5
		0·5	80·2	53·6	−4·3	4·1
	2·0	0·1	77·9	57·1	−4·2	4·0
		0·3	79·6	56·0	−4·4	4·0
		0·5	80·7	54·1	−4·3	3·8

Table 4. DSC transition-midpoint temperatures extrapolated to zero scan-rate and mean values of ΔH averaged over heating and cooling scans for Methocel samples measured at the concentrations and scan-rates shown in Table 3

Methocel sample	T_m (°C) at zero scan-rate		Mean ΔH (J g^{-1})
	Heating	Cooling	
A4M	59·1	38·6	15·9 ± 0·5
E4M	64·3	51·5	14·6 ± 0·3
F4M	65·7	51·5	15·3 ± 0·5
K4M	76·5	57·6	4·2 ± 0·2

SOLUTION RHEOLOGY

As illustrated in Fig. 16, the shear-rate dependence of steady-shear viscosity (η) and frequency dependence of complex dynamic viscosity (η^*, measured in the linear viscoelastic region at low strain) superimpose closely for HPMC, indicating the absence of enthalpic interactions between the individual species present in solution. The form of shear-thinning, however, is different from that of underivitised polysaccharide coils.

As discussed previously, flow-curves for normal polysaccharide solutions follow the general relationship between viscosity and shear rate described by eqn (2), giving linear plots of η versus $\eta\dot{\gamma}^p$ for $p = 0{\cdot}76$. The corresponding plots for HPMC show obvious curvature (Fig. 17(a)) but good linearity is obtained with $p = 0{\cdot}56$ (Fig. 17(b)), as was also found for A4M (Haque & Morris, 1993).

When measured viscosities are expressed as a fraction of the maximum 'Newtonian' viscosity at low shear rate (i.e. as η/η_0) and applied shear-rates are similarly expressed as a fraction of $\dot{\gamma}_{1/2}$ (the shear-rate required to reduce η to $\eta_0/2$) then, as shown in Fig. 18(a), the flow

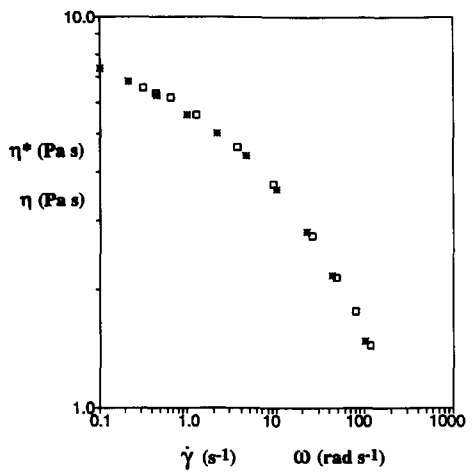

Fig. 16. Cox–Merz comparison of the shear rate ($\dot{\gamma}$) dependence of steady-shear viscosity (η; □) and the frequency (ω) dependence of complex dynamic viscosity (η^*; *), illustrated for 2% (w/v) E4M at 25°C.

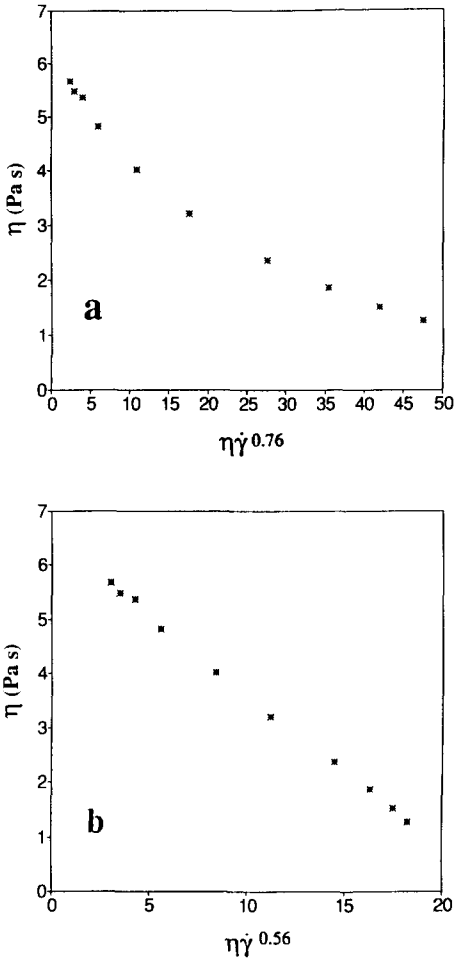

Fig. 17. Shear thinning behaviour of 2% (w/v) E4M plotted as η versus $\eta\dot{\gamma}^p$ for (a) $p = 0{\cdot}76$ and (b) $p = 0{\cdot}56$.

curves for A4M, E4M, F4M and K4M converge to a single 'master plot' (as would be expected from all four samples having the same best-fitting value of p). Similar convergence is observed for the frequency dependence of η^* (Fig. 18(b)). Thus, different Methocels show an identical form of shear thinning, but one that is significantly different from the invariant behaviour of entangled polysaccharide coils. The obvious conclusion is, of course, that the 'bundle' structure proposed for A4M (Haque & Morris, 1993) is also present in solutions of E4M, F4M and K4M. Confirmatory evidence from other techniques is given in the following sections.

OPTICAL ROTATION

Figure 19 shows the changes in optical rotation (365 nm) observed on heating and cooling solutions of K4M (1% (w/v)) and E4M (1 and 0·5% (w/v)). As found for A4M (Haque & Morris, 1993), there is clear evidence of a co-operative conformational transition, with appreciable thermal hysteresis, consistent with

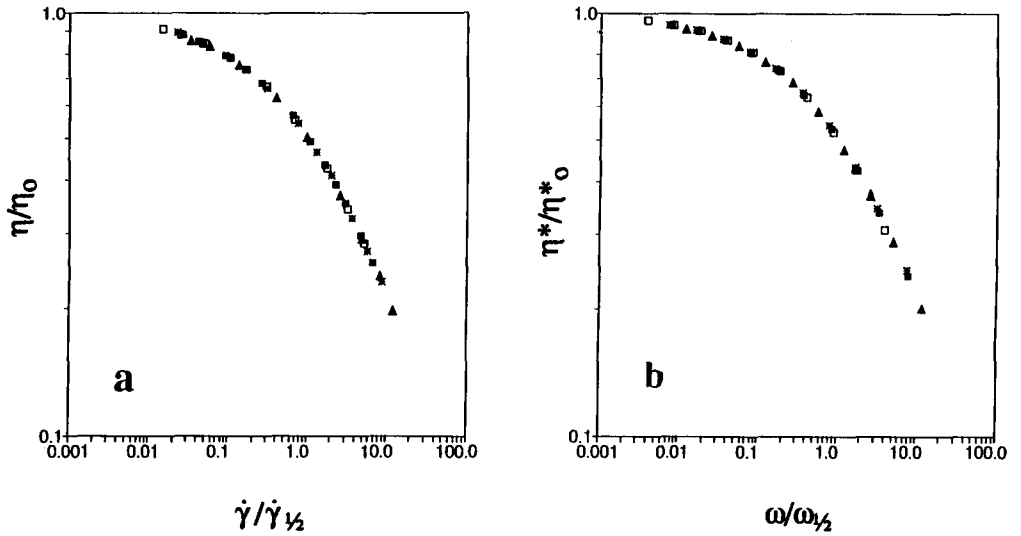

Fig. 18. Generalised shear thinning behaviour of Methocel samples A4M (■), E4M (▲), F4M (□) and K4M (*); (a) steady-shear viscosity; (b) complex dynamic viscosity; $\eta = \eta_0/2$ at $\dot{\gamma} = \dot{\gamma}_{1/2}$; $\eta^* = \eta^*_0/2$ at $\omega = \omega_{1/2}$.

melting and re-formation of the postulated cellulosic bundles. The readings obtained for E4M at 0·5% (w/v) follow the same temperature course as those at 1·0% (w/v), consistent with the absence of any detectable concentration dependence in the temperature of DSC transitions (Fig. 15) or rheological changes (Fig. 10) and show, to within experimental error, the expected two-fold reduction in magnitude.

The midpoint-temperatures for the optical rotation transitions (Table 5) fall in the same order as the thermogelation processes shown in Fig. 6 (A4M < E4M < K4M). The increase in T_m is accompanied by a systematic increase in the extent of thermal hysteresis and by a systematic decrease in the overall magnitude of optical-rotation change per unit concentration of polymer ($\Delta OR/c$; Table 5).

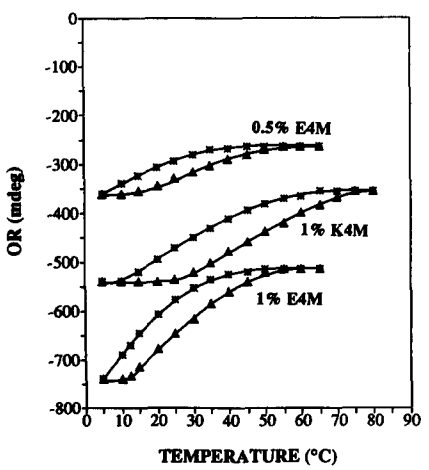

Fig. 19. Temperature dependence of optical rotation (365 nm; 10 cm pathlength) for E4M (0·5 and 1·0% (w/v)) and K4M (1·0% (w/v)) on heating (▲) and on cooling (*).

NUCLEAR MAGNETIC RESONANCE

Figure 20 shows the ^{1}H-NMR spectrum obtained for K4M (1% (w/v)) in D_2O) at 25°C (in the chemical-shift range below the HOD peak at ~4·7 ppm). The main difference from the spectra obtained for A4M (Haque & Morris, 1993) is the appearance of a new resonance at ~1·1 ppm. This comes from the methyl groups of hydroxypropyl substituents (which are attached to carbon rather than oxygen, and therefore have a different chemical shift to *O*-methyl groups). Since the hydroxypropyl MS value for K4M is 0·22 (Table 2), and each methyl group contains three protons, the peak at $\delta = 1{\cdot}1$ ppm should have an integrated intensity corre-

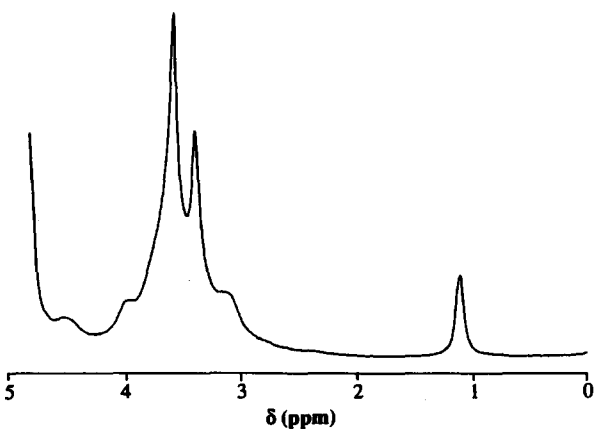

Fig. 20. Illustrative high-resolution ^{1}H-NMR spectrum (200 MHz) for K4M (1%(w/v) in D_2O) at 25°C. The signal at $\delta \approx 1{\cdot}1$ ppm is from methyl protons of hydroxypropyl substituents. The resonances between ~2·0 and ~4·3 ppm are from *O*-methyl groups and non-anomeric protons of the sugar rings. The intense signal whose onset is shown at ~4·5 ppm comes predominantly from HOD, and masks the resonance from anomeric protons.

Table 5. Optical rotation transitions for Methocel samples

Material	T_m(°C)		Hysteresis (°C)	$\Delta OR/c$ (365 nm) (deg ml g^{-1})
	Heating	Cooling		
A4M	24	15	9	27
E4M	29	18	11	21
K4M	48	31	17	18

sponding to 0·66 protons per sugar ring if the polymer is fully disordered.

The hydroxypropyl substituents ($-CH_2-CHOH-CH_3$) contain three further non-exchangeable protons. These will give resonances in the spectral region between ~2·0 and ~4·3 ppm, along with the protons of the methoxyl substituents (DS = 1·40; Table 2) and the six non-exchangeable, non-anomeric protons of each glucose residue. At full visibility, the intensity of the signal in this region would therefore correspond to 6 + 3DS + 3MS = 10·86 protons per sugar ring. The proportion of these maximum calculated intensities observed experimentally at different temperatures was determined, as before (Haque & Morris, 1993), by comparison with the signal from a pyrazine standard calibrated against a 5% solution of dextran. The results are shown in Fig. 21, in comparison with the corresponding values for A4M.

As would be anticipated from the temperature course of thermogelation (Fig. 6), loss of NMR intensity occurs at higher temperature for K4M than for A4M. At all temperatures the hydroxypropyl groups give a higher fractional visibility than the rest of the polymer, indicating either that a proportion of these substituents remain free to rotate on the periphery of otherwise rigid structures and/or that regions with a high content of hydroxypropyl groups have greater segmental mobility. In particular, more than 20% of the hydroxypropyl signal remains visible in the gel state at high temperature.

In the solution state at 25°C, ~30% of the hydroxypropyl signal and ~40% of the signal from the polymer backbone and methoxyl substituents is 'missing' from the high-resolution spectrum, showing that at least a third of the polymer is conformationally immobile. About half this missing signal becomes visible in the initial stages of heating, indicating partial dissociation of the structures present at lower temperature. The detectable signal from K4M is substantially higher than that of A4M at all stages of thermogelation and dissociation, again indicating that the presence of a few hydroxypropyl groups can seriously inhibit association and packing of methylcellulose chains.

DISCUSSION

The results presented above confirm and extend the conclusions drawn in the preceding paper (Haque & Morris, 1993). It is clear from the NMR evidence that Methocels do not exist in solution as disordered coils, but have substantial structural rigidity. Departures from 'random coil' geometry are also evident in the anomalous shear-rate dependence of viscosity shown in Fig. 17, but the common form of shear thinning observed (Fig. 18) for different Methocel samples suggests closely similar macromolecular organisation in all cases.

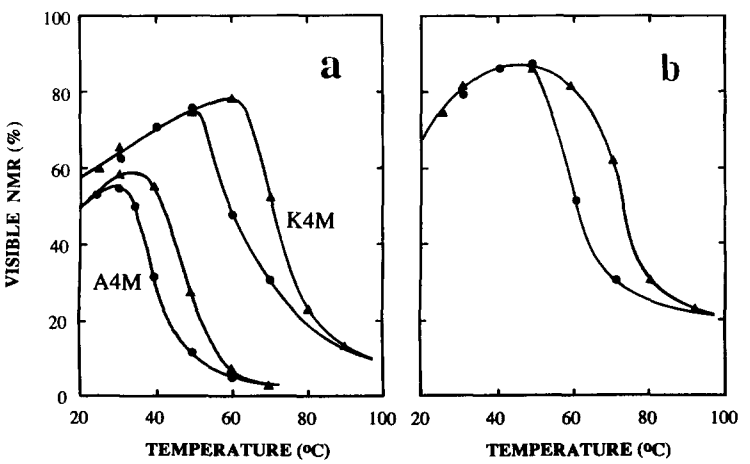

Fig. 21. Changes in the percentage of detectable high-resolution ^{1}H-NMR signal for Methocel samples (1% (w/v) in D_2O) on heating (▲) and cooling (●). (a) *O*-Methyl and non-anomeric carbohydrate protons of A4M and K4M; (b) methyl protons from the hydroxypropyl groups of K4M.

Partial melting of the structures present in solution is demonstrated by an initial increase in detectable high-resolution NMR on heating (Fig. 21), accompanied by a sigmoidal change in optical rotation (Fig. 19). Both are fully reversible on cooling, but with substantial thermal hysteresis. The proposal (Haque & Morris, 1993) that it is this precursor stage that imposes hysteresis on the thermogelation and dissociation processes at higher temperature is supported by the observation that Klucel, which shows no evidence of residual cellulosic structure in solution, also shows little, if any, hysteresis.

Incorporation of a small proportion of hydroxypropyl substitution in methylcellulose appears to inhibit intermolecular association, since:

(1) the intensity of visible ^{1}H-NMR signal in the solution state is greater (Fig. 21),
(2) thermogelation does not occur until higher temperature (Fig. 6), and
(3) the resulting gels are substantially weaker (Fig. 8).

The decrease in optical-rotation change (Table 5) is also consistent with a smaller proportion of ordered structure in solution.

Inhibition of thermogelation may be explained, at least in part, by the more polar (and therefore less hydrophobic) character of the hydroxypropyl group in comparison with methyl substituents. The inhibitory effect on chain packing at lower temperature is likely to arise from a combination of the internal flexibility of the hydroxypropyl group (imposing an entropic restriction on ordered association) and its physical size, which may be difficult to accommodate within a close-packed aggregate. The same entropic and packing considerations would, of course, also apply to formation of the gel network at high temperature. The resistance of hydroxypropyl groups to incorporation within ordered structures is demonstrated directly by their proportion of visible NMR signal (Fig. 21), which is appreciably greater than that of the polymer to which they are attached.

Figure 22 gives a general overview of the thermogelation behaviour of HPMC (illustrated for K4M). The involvement of two separate processes over different ranges of temperature is clear. The low-temperature process is marked by an increase in detectable ^{1}H-NMR, a sigmoidal change in optical rotation, and an initial decrease and subsequent increase in G'. As in the discussion of methylcellulose gelation (Haque & Morris, 1993), these changes are interpreted in terms of progressive disruption of cellulosic 'bundles', resulting in a tenuous network of swollen clusters with hydrophobic substituents surrounded by sheaths of structured water. The second process — giving visual opacity, thermal transitions in DSC, loss of detectable NMR, and development of stable network structure — is attributed to disruption of the water 'cages', with consequent hydrophobic association of the polymer chains.

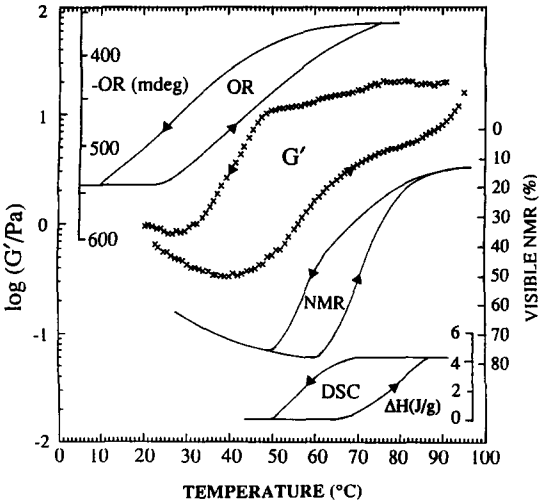

Fig. 22. Direct comparison of the temperature course of changes in chain conformation (OR), structural rigidity (G'), absorption or emission of heat (DSC) and conformational mobility (NMR) for 1% (w/v) K4M.

ACKNOWLEDGEMENTS

We thank Dr N. Sarkar (Dow Chemical Company) and Dr E. Just (Hercules) for information on the chemical composition of the samples studied, and also The British Council for the award of a Study Fellowship to one of us (A.H.).

REFERENCES

Franks, F. (1983). *Water.* Royal Society of Chemistry, London.
Greminger, G.K., Jr & Savage, A.B. (1973). In *Industrial Gums,* eds. R.L. Whistler & J.N. BeMiller. Academic Press, New York, pp. 619–47.
Grover, J.A. (1986). In *Food Hydrocolloids, Vol. 3,* ed. M. Glicksman. CRC Press, Boca Raton, FL, pp. 121–54.
Haque, A. & Morris, E.R. (1993). *Carbohydr. Polym.,* **22,** 161–73, (this issue).
Haque, A., Morris, E.R. & Richardson, R.K. (1993). In *Frontiers in Carbohydrate Research 3,* eds T. Eads, R.P. Millane, J.N. BeMiller & R. Chandrasekaran. Elsevier, New York, (in press).
Haque, A., Jones, A.K., Richardson, R.K. & Morris, E.R. (1994). In *Gums and Stabilisers for the Food Industry 7,* eds G.O. Phillips, P.A. Williams & D.J. Wedlock, IRL Press, Oxford, (in press).
Jones, A.K. (1992). Hydrophobicity in polysaccharide gelation. PhD thesis, Cranfield Institute of Technology, Bedford, UK.
Klug, E.D. (1971). *J. Polym. Sci. C,* **36,** 491–508.
Morris, E.R. (1984). In *Gums and Stabilisers for the Food Industry 2,* eds G.O. Phillips, D.J. Wedlock & P.A. Williams. Pergamon Press, Oxford, UK, pp. 57–78.
Morris, E.R. (1990). *Carbohydr. Polym.,* **13,** 85–96.
Robitaille, L., Turcotte, N., Fortin, S. & Charlet, G. (1991). *Macromolecules,* **24,** 2413–18.
Sarkar, N. (1979). *J. Appl. Polym. Sci.,* **24,** 1073–87.
Tanford, C. (1980). *The Hydrophobic Effect: Formation of Micelles and Biological Membranes.* John Wiley, New York.